Sucker-Rod Pumping of Oil Wells: Modeling and Process Control

LUIZ H. S. TORRES, LEIZER SCHNITMAN
Universidade Federal da Bahia
Centro de Capacitação Tecnológica em Automação Industrial (CTAI)
Rua Aristides Novis, n 02, Escola Politécnica
segundo andar, 40.210-630, Salvador, Bahia
(Tel/fax number: +55-71-3283-9755)
BRAZIL
luizhtorres@gmail.com, leizer@ufba.br

Abstract: This paper presents an robust adaptive controller being used to address some of the uncertainties in the system model, including unmodeled dynamics, parameter variations, and the presence of perturbations in the automatic control system of a real sucker-rod pump. The results show that the control system is able to satisfactorily handle uncertainties and variations, such as in the pumped fluid composition, a very common situation in real production fields. Experimental tests conducted in a real plant validate the robustness of the control algorithm.

Key–Words: Adaptive control, Robust control, Sucker-rod pumping, Smart oil fields, System automation, Variable structure control

1 Introduction

The sucker-rod pumping system is the artificial lift method most commonly used in the on-shore petroleum industry, due to the simplicity of the required equipment and facilities [1]. This system is historically considered the first method among oil well lift systems. It is widely used in shallow wells with low to medium flow rates. Studies have shown that the method's popularity is also due to its low investments and maintenance costs and to its ability to accommodate different fluid compositions and viscosities at a wide range of temperatures [2].

Although this lift method is well known and widely used, there are still some circumstances in which improvements to the technology are possible, especially when considering process control strategies for the pumping unit to improve system productivity. The development of low cost sensors has made possible the measurement of bottomhole variables to assist in monitoring production and the application of new control strategies [3, 4, 5]. The concept of smart wells, using the process of smart completion, describes a set of technologies developed for the automation of wells with the goal of improving the operation of oil production fields [6]. Smart completion comprises the installation of subsurface equipment, such as control valves and instruments, to provide digital measurements of variables such as pressure, temperature and flow [7, 8]. The smart field technology utilizes smart well systems to monitor and control equipment at the surface, bottomhole and reservoir to optimize the operation of the entire field [9, 10, 11]. As a result, a new paradigm has been developed for systems automation of oil production [12, 13, 14].

Simulation software and models have aided studies of the modeling and design of control systems for sucker-rod pumping systems and other artificial lift methods [15, 16, 17]. However, most of these simulations and models have been limited to theoretical studies that do not take into account the practical situations encountered in real production fields. Additionally, in the process control of the pumping unit, the presence of uncertainties in the parameters, parameter variations, unmodeled dynamics, and perturbations present challenges in the design of the control system, and they can jeopardize the performance of a conventional proportional integral derivative (PID) controller. Thus, and as it can be seen in some similar situations in literature [18, 19], it is necessary a robust and adaptive approach to face this scenario. [20] presented an initial proposal for the mathematical modeling of a real sucker-rod pumping and an adaptive control algorithm was briefly described that addressed some of the challenges that this type of system can face in real production oil fields. In the present paper, a model based on first-principle modeling is presented and the mathematical description of the control algorithm and its results obtained are detailed.

This paper is organized as follows: Section 2 presents a typical sucker-rod pumping system and some of the operational aspects of this artificial oil lift method. Section 3 presents a mathematical model of a real sucker-rod pumping system. Section 4 is devoted to a brief description of the algorithm for the adaptive controller used. The results obtained from the adaptive controller are presented and its performance demonstrated in section 5. Section 6 presents the conclusions.

2 Sucker-Rod Pumping System

In this artificial lift method, the rotary movement of a prime mover (either an electric motor or a combustion engine) localized at the surface of the pumping unit is converted to the reciprocating movement of a rod string. This column transmits the reciprocating movement to the pump components located at the bottom of the well, which are responsible to elevating the fluid from the reservoir to the surface. The sucker-rod pumping system can be divided into downhole and surface elements (see Fig.1).

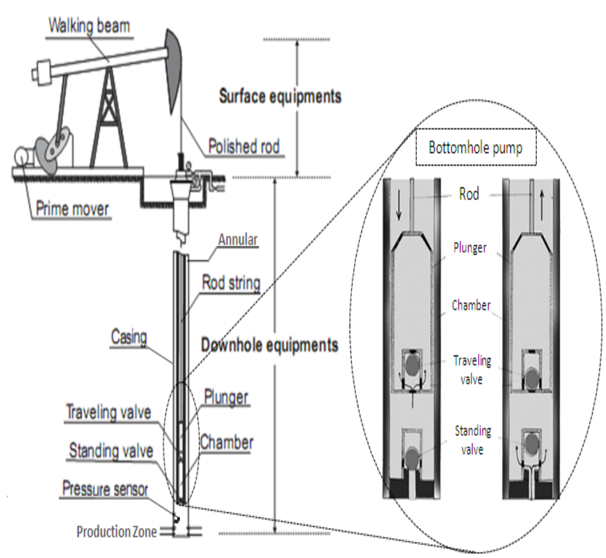

Figure 1: Components of a sucker-rod pumping system.

The rod string is the link between the pumping unit located on the surface and the bottomhole pump. The bottomhole pump is a simple type of positive-displacement reciprocating pump in which the fluid is displaced in one direction of the alternating movement. The function of the bottomhole pump is to provide energy to the fluid in the reservoir [1]. In Fig.2, a schematic of the bottomhole is presented. The annular well and pump inlet level are also shown.

The pumping cycle due to the relative motion of the valves affects the bottomhole pressure. The oil production is controlled by varying the prime mover

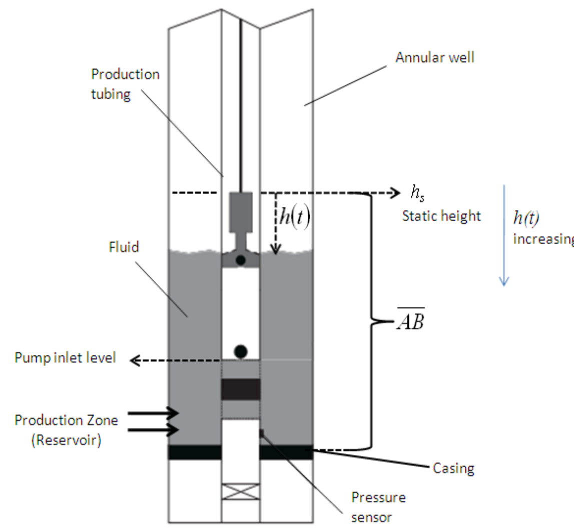

Figure 2: Bottomhole schematic with sucker-rod pumping system.

velocity, which in turn varies the pumping speed, measured in cycles per minute (CPM). In this control strategy the variable speed drive (VSD), technique is used. This allows the pumping speed to be adjusted through a frequency inverter device [21, 17]. It is important to note that the production performance is affected by the annular fluid level, and operating at the minimum possible annular level (i.e., the minimum bottomhole pressure) maximizes the reservoir oil outflow [16]. In the design of a control system to increase oil production, a dynamic model of the sucker-rod pumping system may relate the pumping speed of the unit to the fluid level in the annular well. The dynamic model may also reveal the relationship between the model parameters and the real process. According to the literature [22, 16], these parameters are usually related to sources such as the fluid characteristics in the well, the environmental properties at the bottom of the hole, the electrical devices, and the mechanical assembly.

3 System Modeling

In systems that use sucker-rod pumps, it is often desirable for an operating range on the downhole fluid level to be very close to the pump inlet level (as showed in Fig.2). This operating range is characterized by complete pump filling with the minimum possible bottomhole pressure. This produces the minimum back pressure in the production zone of the reservoir and in turn increases oil production [16]. In the Laboratório de Elevação Artificial (LEA; in English, the Artificial Lift Lab) at the Universidade Federal da Bahia (UFBA), there is a real plant of a sucker-rod pump with an artificial well of 32 m height, fully instrumented, with full access and a visible bottomhole. All components of this equipment are industrial grade and the plant includes a supervisory system for data acquisition and control. A schematic of this well is presented in Fig.3 and Fig.4.

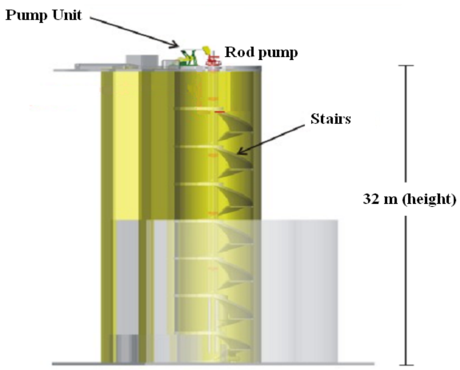

Figure 3: Infrastructure and layout.

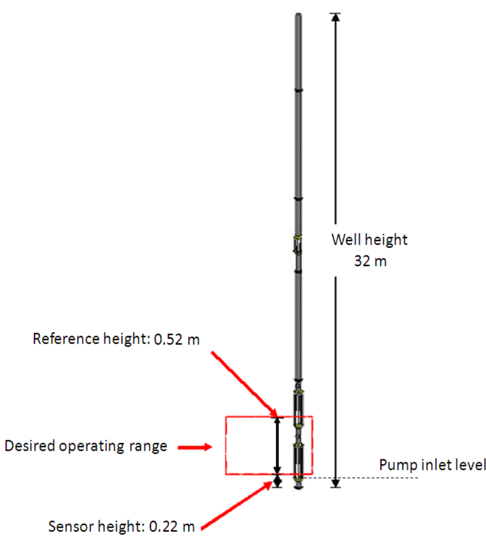

Figure 4: Well schematic of the rod pump in the LEA.

In modeling procedures, variables (i.e., input and output signals) are often used that measure a deviation from a reference or a nominal operating point. In this work, a reference is chosen by considering a desired operating range and the pump inlet level. A schematic of the well with the chosen reference and operating range is shown in Fig.4. It is important to note that the production performance is associated with the annular fluid level. Therefore, a dynamic model of sucker-rod pumping may be developed by relating the pumping speed of the unit with the fluid level in the annular well in order, for example to assist in system monitoring or for control purposes. Consequently, in this model, the level in the annular well $h(t)$ (measured in meters) is considered as the process output and the pumping speed $N(t)$ (measured in CPM) as the process input.

It is possible to obtain the volumetric balance of the liquid drainage from the annular well. It can be written as follows,

$$q_a(t) + q_r(t) = q_p(t) \, , \tag{1}$$

where $q_a(t)(t)$ is the flow (in cubic meter per day, m^3/d) from anullar well to the production tubing (where is located the bottomhole pump), $q_r(t)$ is flow (in m^3/d) from the reservoir to the production tubing, and $q_p(t)$ is the pump flow (in m^3/d). The flow from anullar well to the production tubing is defined as,

$$q_a(t) = A_a \cdot \frac{d}{dt}(h(t)) \, , \tag{2}$$

where $\frac{d}{dt}(h(t))$ is the level rate in the anullar well and A_a is the anullar cross-sectional area (in square inches, in^2). This area is calculated as follow,

$$A_a = \frac{\pi}{4} \cdot ((D_i^c)^2 - (D_e^t)^2) \, , \tag{3}$$

where D_i^c is the internal diameter (in in) of the casing tubing, and D_e^t is the external diameter (in in) of the production tubing. The flow from the reservoir to the production tubing is stated as,

$$q_r(t) = PI \cdot (P_s - P_w(t)) \, , \tag{4}$$

where PI is called productivity index (in $\frac{m^3/d}{kgf/cm^2}$), P_s is the static pressure (in kgf/cm^2), and $P_w(t)$ is the well flowing pressure (in kgf/cm^2) (also called downhole pressure). Equation (4) also express a relationship between the oil production rate from the reservoir $q_r(t)$ and the downhole pressure $P_w(t)$. This relationship is called inflow performance relationship (IPR). In order to obtain initially a simple and representative reference-model of the actual system in LEA, the relationship presented in Eq.(4) assumes a single-phase flow and the pressure in the porous media (reservoir) is above the bubble point pressure (saturation pressure). Thus, the flow $q_r(t)$ varies linearly with the downhole pressure $P_w(t)$. Fig.5 shows the linear IPR graph.

The static pressure P_s is given by,

$$P_s = P_c^s + \gamma_f \cdot \overline{AB} \, , \tag{5}$$

where P_c^s is the casing pressure (in kgf/cm^2) in static conditions (i.e.: the pumping system is turned off and, thus, there is no production from the well), γ_f is the specific weight (in Newton per cubic meter, N/m^3) of the fluid, and $\overline{AB}$ is the length (in m) between the static level h_s and the casing (as shown in Fig.2). In this work the pressure of the gas column on the fluid

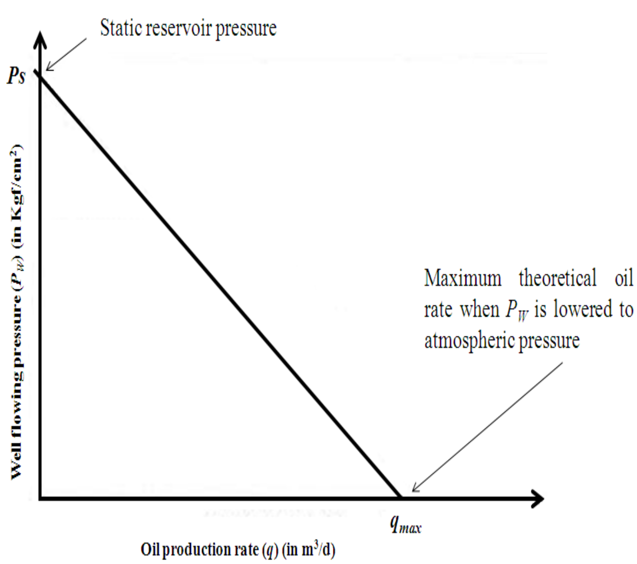

Figure 5: The inflow performance relationship.

in the annular well is not considered. The well flowing pressure $P_w(t)$ is given by,

$$P_w(t) = P_c^d + \gamma_f \cdot (\overline{AB} - h(t)) \; , \tag{6}$$

where P_c^d is the casing pressure (in kgf/cm^2) in dynamics conditions (i.e.: the pumping system is turned on and, thus, there is production from the well), and $h(t)$ is the level as indicated in Fig.2. It is assumed here $P_c^s \approx P_c^d$. The flow from the reservoir to the production tubing in Eq.(4) can be rewritten considering the Eq.(5) and Eq.(6).

$$q_r(t) = PI \cdot \gamma_f \cdot h(t) \; . \tag{7}$$

Thus, the Eq.(1) can be rewritten as follow,

$$A_a \cdot \frac{d}{dt}(h(t)) + PI \cdot \gamma_f \cdot h(t) = q_p(t) \; , \tag{8}$$

$$\frac{d}{dt}(h(t)) = -\frac{PI \cdot \gamma_f}{A_a} \cdot h(t) + \frac{1}{A_a} \cdot q_p(t) \; . \tag{9}$$

It could be observed that the dynamic model in Eq.(9) is a linear relationship given by a first order ordinary differential equation. According to [23], the pump flow (in m^3/d) of a sucker-rod pump can be given by,

$$q_p(t) = 2.36 \times 10^{-2} \cdot \eta \cdot A_p \cdot S_p \cdot N(t) \; , \tag{10}$$

where η is the volumetric efficiency of the pump (in %), A_p is the cross sectional area of the pump plunger (in in^2), S_p is the plunger stroke length (in in), and $N(t)$ is the pumping speed (in cycles per minute). The value of the volumetric efficiency of the pump η is normally in the range of 70 and 80. Finally, the level rate into the anullar can be calculated as a function of the pumping speed $N(t)$ as follow,

$$\begin{aligned} \frac{d}{dt}(h(t)) = \; & -\frac{PI \cdot \gamma_f}{A_a} \cdot h(t) + \\ & + \frac{(2.36 \times 10^{-2} \cdot \eta \cdot A_p \cdot S_p)}{A_a} \cdot N(t) \; . \end{aligned} \tag{11}$$

As shown in the Fig.2 the level in the anullar is measured by using a pressure sensor. The pump speed can be varied by using a frequency inverter on the surface facilities.

4 Robust Adaptive Control Technique

In systems that use sucker-rod pumps, it is often desirable for the operating range on the downhole fluid level to be very close to the pump inlet level. In this work, a robust adaptive controller called indirect variable structure model reference adaptive control (IVS-MRAC) is applied to a sucker-rod pump. It is expected that the controller operate inside the desired range on the downhole fluid level. Moreover, the controller must be able to adapt its parameters and demonstrate robustness in the case of process changes, uncertainties, variations, unmodeled dynamics, and perturbations in the system. It is essential to remark that such conditions are physical quantities of a sucker-rod pumping. Variations, for example, can be the result of a change in the composition of the fluid flow produced (water, oil and/or gas), or in some parameters of the system well-reservoir, such as, Basic Sediment and Water (BS & W), Gas-Oil Ratio (GLR), Gas-Oil Ratio (GOR), specific weight of the fluid, and the Productivity Index (*PI*) [2]. There are also operational problems, that disrupt the system and may compromise the productivity of the method, such as, fluid pound phenomenon [16], leaks fluid in the traveling and/or standing valves or in the production tubing, low efficiency of the system due to incomplete filling of the pump, and a failure of the electric power system frequency inverter.

The IVS-MRAC controller was initially proposed in [24] as an alternative to the direct approach, called VS-MRAC [25]. Its mathematical description, and the stability analysis and its proof in the presence of unmodeled dynamics and perturbations for the case of relative degree one, can be found in [26]. A simplified version, including the practical application of the

IVS-MRAC controller to the speed control of a three-phase induction motor, can be found in [27].

This technique was developed based on the indirect MRAC approach (called I-MRAC). The classic I-MRAC method is one of the primary techniques in adaptive control [28, 29], and it is still generating new research and publications [30]. The desired response is provided by a reference model, and the control objective is to minimize the error between the system under control and a model reference output. In the IVS-MRAC scheme, there are new features added to the I-MRAC approach. By using the sliding mode control based on variable structure control (VSC) [31], the I-MRAC method is associated with fast transient and good robustness to parameter uncertainties, variations, and perturbations. The IVS-MRAC scheme estimates the plant parameters instead of using the controller parameters.

The IVS-MRAC controller provides a straightforward design for the relay amplitudes used in the switching laws of the control algorithm [27], because the relays are directly associated with the plant parameters. These parameters, in turn, represent the relationships among the physical parameters of the system, such as the resistances, capacitances, moments of inertia, and friction coefficients, that have uncertainties that are relatively easily determined. The block diagram shown in Fig.6 illustrates the general concept of the IVS-MRAC scheme.

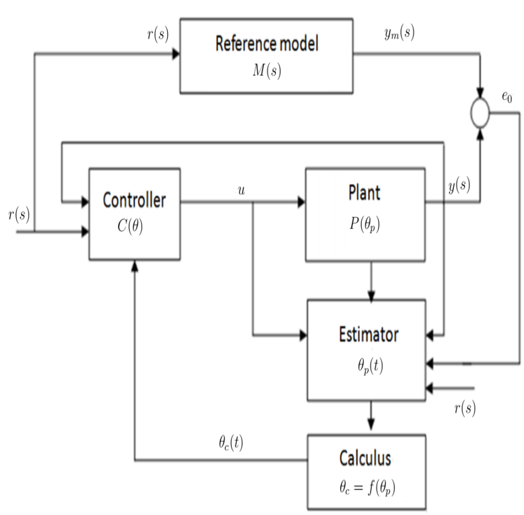

Figure 6: The general concept of the IVS-MRAC scheme.

The model plant, $P(\theta_p)$, is parameterized in relation to the vector $\theta_{\mathbf{p}}$. An estimator generates $\theta_{\mathbf{p}}(\mathbf{t})$ by processing the input signal u and the output signal y. The estimate $\theta_{\mathbf{p}}(\mathbf{t})$ specifies a model characterized by $\hat{P}(\theta_p(t))$ that, for the purposes of the controller design, is treated as the true model of the plant at the instant t. The latter is used to calculate the controller parameters $\theta_c(t)$ from the algebraic equation $\theta_c(t) = f(\theta_p(t))$. The control law $C(\theta)$ and the equation $\theta_c = f(\theta_p)$ are calculated to meet the performance requirements for the model $P(\theta_p)$.

4.1 Mathematical Description

The mathematical development of the IVS-MRAC scheme related to adaptation of the controller algorithm to this specific problem will be presented here. The transfer function of the plant can be described as follows:

$$P(s) = k_p \cdot \frac{n_p(s)}{d_p(s)} \,, \tag{12}$$

where k_p is the high frequency gain. For the case of relative degree one ($n^* = 1$), n_p and d_p are monic polynomials set to be,

$$n_p(s) = s^{n-1} + \sum_{i=1}^{n-1} \beta_i \cdot s^{n-1-i} \,, \tag{13}$$

$$d_p(s) = s^n + \alpha_1 \cdot s^{n-1} + \sum_{i=1}^{n-1} \alpha_{i+1} \cdot s^{n-1-i} \,. \tag{14}$$

The desired response, given by the transfer function of the model reference signal, can be written as follows:

$$\frac{y_m(s)}{r(s)} = M(s) = k_m \cdot \frac{n_m(s)}{d_m(s)} \,, \tag{15}$$

where y_m is the model reference output. It is assumed the reference input r is a piecewise continuous signal and uniformly bounded. The polynomials n_m and d_m are similarly defined as the following polynomials of the plant:

$$n_m(s) = s^{n-1} + \sum_{i=1}^{n-1} \beta_{m,i} \cdot s^{n-1-i} \,, \tag{16}$$

$$d_m(s) = s^n + \alpha_{m,1} \cdot s^{n-1} + \sum_{i=1}^{n-1} \alpha_{m,i+1} \cdot s^{n-1-i} \,. \tag{17}$$

The vector of plant parameters, which are assumed to be known, is set to be

$$\theta_{\mathbf{p}} = [k_p, \beta^T, \alpha_1, \alpha^T]^T \,, \tag{18}$$

where $\beta \in R^{n-1}$ contains the elements of $\beta_i (i = n-1, \ldots, 1)$, $\alpha_i \in R$ is element α_1 in Eq.(14), $\alpha \in R^{n-1}$ contains the elements of $\alpha_{i+1} (i = n-1, \ldots, 1)$ in

Eq.(14), and, in the same way, one sets β_m, $\alpha_{m,1}$ and α_m, in Eq.(16) and Eq.(17). When the plant parameters are unknown or known with uncertainties, the estimated vector is given by

$$\hat{\theta}_\mathbf{p} = [\hat{k}_p, \hat{\beta}^T, \hat{\alpha}_1, \hat{\alpha}^T]^T \ . \tag{19}$$

The following assumptions regarding the plant and the reference model are made in accordance with [27]:

A1 the plant is completely observable and controllable with degree $(d_p) = n$ and degree $(n_p) = n-1$, where n is known;

A2 $sgn(k_p) = sgn(k_m)$ (positive, for simplicity);

A3 $n_p(s)$ is Hurwitz, *i.e.*, $P(s)$ is minimum phase;

A4 $M(s)$ has the same relative degree as $P(s)$ and is chosen to be strictly positive real (SPR);

A5 upper bounds for the nominal plant parameters are known.

For a first-order system, such as the sucker-rod pumping system studied, the vector of estimated parameters can be rewritten as

$$\hat{\theta}_\mathbf{p} = [\hat{k}_p, \hat{\alpha}_1,]^T \ . \tag{20}$$

The error equation between the plant response and the reference model output (i.e., the desired response) is given by

$$e_0 = y - y_m \ . \tag{21}$$

If the previous assumptions are satisfied, the matching condition is met, *i.e.*, $y \to y_m$. The control law u can be rewritten as

$$u = \theta_n \cdot y + \theta_{2n} \cdot r \ , \tag{22}$$

$$\theta_n = \frac{\hat{\alpha}_1 - \alpha_{m,1}}{\hat{k}_p} \ , \tag{23}$$

$$\theta_{2n} = \frac{k_m}{\hat{k}_p} \ . \tag{24}$$

The controller parameters are updated using the estimates of the plant parameters, characteristic of the IVS-MRAC approach. The estimates, in turn, are obtained according to the original laws as shown in [27]:

$$\hat{k}_p = k_p^{nom} - \overline{k}_p \cdot sgn(v_{av}) \ , \tag{25}$$

$$\hat{\alpha}_1 = -\overline{\alpha}_1 \cdot sgn(e_0\zeta_1) \ , \tag{26}$$

where *sgn* is the signum function and ζ_1 is an auxiliary signal. In this work, this signal is defined as $\zeta_1 = y$. The values of k_p^{nom}, $\overline{k}_p$, and $\overline{\alpha}_1$ are constants. The values $\overline{k}_p$ and $\overline{\alpha}_1$ are associated with the relay sizing in the switching laws in Eq.(25) and Eq.(26). From Eq.(25), the presence of k_p^{nom} (the positive and nominal value of k_p) is justified to prevent the estimate of the high frequency gain of the plant $\hat{k_p}$ from becoming negative, a situation that would violate assumption *A2*. Finally, the sufficient conditions to design the relay amplitudes and, in turn, to obtain the sliding mode are

$$\overline{k}_p > |k_p - k_p^{nom}| \text{ com } k_p^{nom} > \overline{k}_p \ , \tag{27}$$

$$\overline{\alpha}_1 > |\alpha_1| \ . \tag{28}$$

The argument v_{av} in Eq.(25) is a mean value first-order filter with a time constant τ that it is sufficiently small (i.e., $\tau \to 0$). It can be seen to represent inherent unmodeled dynamics that could influence the system stability. A stability proof of the IVS-MRAC scheme incorporating this assumption can be found in [26]. The function v_{av} can be set as

$$v_{av} = \frac{1}{\tau \cdot s + 1} \cdot \mathsf{v} \ , \tag{29}$$

where v is an auxiliary signal, defined as $\mathsf{v} = -e_0 \cdot u$.

5 Results

5.1 Simulation Results

The proposed controller for the level control of the fluid in the annular well of a sucker-rod pumping system is implemented as follows. The data used is this work (both in simulation and practical tests) were obtained from the industrial equipment in the laboratory (LEA).

From Eq.(11), Eq.(12) and data from LEA, the continuous-time SISO transfer function of the plant dynamic model is as follows:

Plant $P(s) = k_p \cdot \frac{n_p(s)}{d_p(s)} = \frac{1.509 \times 10^{-3}}{s + 6.739 \times 10^{-2}}$

$\Rightarrow k_p = 1.509 \times 10^{-3}$; $\alpha_1 = 6.739 \times 10^{-2}$

The reference model from Eq.(15) may be chosen as follows:

Reference Model $M(s) = k_m \cdot \frac{n_m(s)}{d_m(s)} = \frac{1.660 \times 10^{-3}}{s + 7.413 \times 10^{-2}}$

$\Rightarrow k_m = 1.660 \times 10^{-3}$; $\alpha_{m,1} = 7.413 \times 10^{-2}$

The plant parameters k_p and α_1 used in the tests were within a 10% uncertainty range of the model reference parameters k_m and $\alpha_{m,1}$. The initial conditions of the plant and the reference model were different to facilitate the observation of the tracking properties. The tests were performed regarding the reference input r as a set of step signals. Parameter values of $k_p^{nom} = 1.509 \times 10^{-3}$ and $\overline{k}_p = 3.018 \times 10^{-4}$ were adopted. The value of $\overline{\alpha}_1$ was chosen based on the value of $|\alpha_1| = 6.739 \times 10^{-2}$, with the inclusion of 10% uncertainty resulting in a value of $\overline{\alpha}_1 = 7.413 \times 10^{-2}$. The time constant τ was adjusted during the tests, and a value of $\tau = 0.001$ was adopted. In these models the level in the annular well (measured in meters) is considered to be the process variable (PV), and the pumping speed (measured in cycles per minute, or CPM) as the manipulated variable (MV). In Fig.7 the reference model output (i.e., the desired response signal) and the process output response are compared. Fig.9 and Fig.8 show the the control effort (related to the variation of the CPM in percent) and error signal (in meters), respectively.

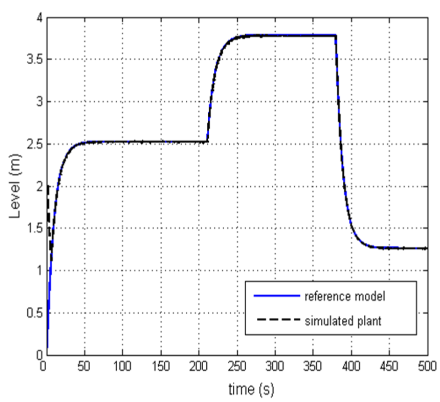

Figure 7: Comparison between the desired response (i.e., the reference model signal) and the process response.

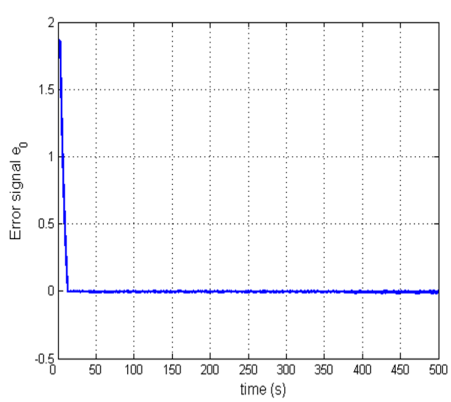

Figure 8: Error signal.

It can be observed in Fig.7 that the reference model (i.e., the desired response) output given was tracked by the process output. The process variable (i.e., the fluid level in the annular well) can be observed in Fig.7 to have no oscillations in the transient,

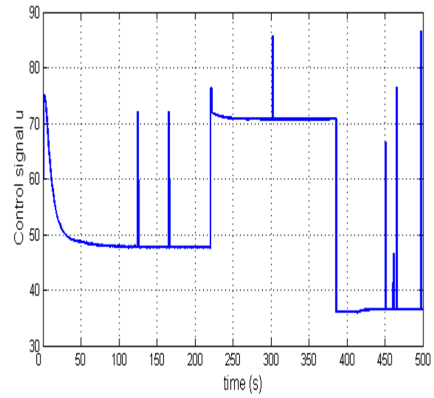

Figure 9: Control effort.

it is stable in the steady state. The control effort is also bounded in Fig.9, and the error in the steady state is small and bounded according to Fig.8. However, Fig.9 indicates an input effort for the proposed controller that in some cases would be considered unacceptable. The chattering phenomenon is an additional difficulty from the emergence of high-frequency unwanted and excessive control activity signals. This phenomenon occurs along the sliding surface due to imperfections introduced by the actual switching mechanisms, such as dead zones, hysteresis, delay, and / or the presence of unmodeled dynamics of the plant [27]. Consequently, strategies for alleviating the chattering phenomenon should be further studied.

5.2 Experimental Results

For the practical test, the IVS-MRAC controller was implemented with the same parameters used in the simulations. The results obtained are shown as follows.

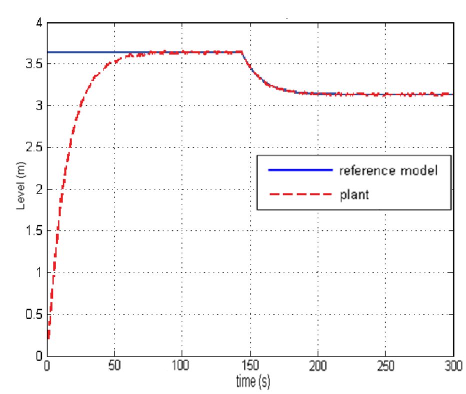

Figure 10: Comparison between the desired and the process responses.

The plant exhibits the same behavior that was ob-

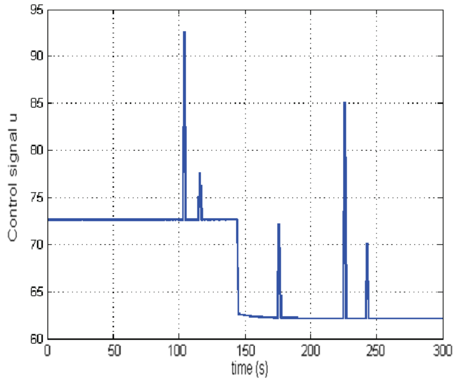

Figure 11: Control effort.

served in simulated environment. In Fig.10 the reference model signal, y_m, is tracked by the plant output y, even when the reference value changes. The transient behaviour is fast, with no oscillations, just as in the simulated results. Fig.11 shows the limited signal control, u, applied to the plant, which is related to the frequency variation (in percentage) associated with the frequency inverter.

Another set of tests was performed to compare the IVS-MRAC controller with a conventional PID controller. In these tests, the objective was to evaluate the robustness and adaptation properties of the controllers. A 15% variation in the parameters k_p and α_1 and a step perturbation of 20% in the MV and PV were introduced. The PID parameters were tuned by root locus method. However, it is important to remark that, in reality, in most of oil production fields no robust tuning method is used to tune the controller. The results are shown in Fig.12 and Fig.13.

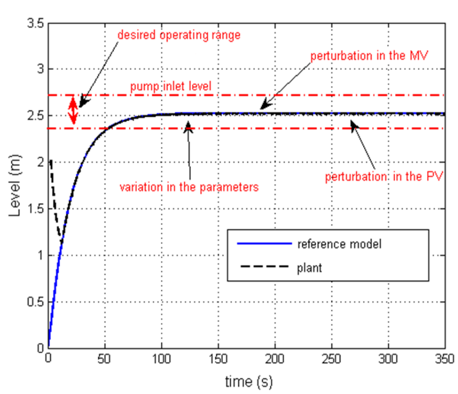

Figure 12: IVS-MRAC subjected to variation in the parameters and presence of perturbations.

It can be seen in these tests that the references are tracked by the controllers. However, in the conventional PID control system (Fig.13), the parameter variations and perturbations cause a performance

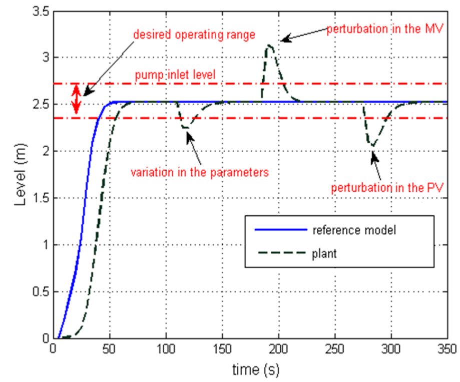

Figure 13: Conventional PID subjected to variation in the parameters and presence of perturbations.

loss, with deviation the process output from the reference and outside the desired operating range. In Fig.12, there is no performance loss, and the IVS-MRAC controller shows robustness. It is important to note that outside the operating range, the oil production is lower. This deviation in the process output can also cause the fluid pound phenomenon [16]. Fluid pound occurs due to the entry of gas into the bottomhole pump, which results when the fluid level is below the pump inlet level. This phenomenon has a negative effect on oil production and maintenance costs. The mechanical fatigue of pump components is also increased by the occurrence of fluid pound. The parameter variations introduced in k_p and α_1 can be related to changes in the fluid composition (water, oil and/or gas), a very common situation in real production fields. The perturbations in the MV, for instance, may be associated with faults in the power supply of the frequency inverter. Perturbations in the PV may be related to leakage in the traveling and/or standing valves [2].

6 Conclusions

In this paper, a mathematical dynamic model was built for a real sucker-rod oil well system and a robust adaptive controller was developed to achieve the control objectives. One of the main challenges that has been repeatedly encountered is the validation of the models for these systems (mostly using techniques such as first-principle modeling tools) because the pumping components, such as the rod string and bottomhole pump, are located in the deep subsurface and without the possibility of easy access. In the plant used in this work, the system is fully instrumented and the bottom is accessible and visible. A contribution of this paper is that the results are not restricted to theoretical models (or simulations) that lack evidence relevant to real production oil fields. The use of the LEA laboratory helps to confirm that the model developed is representative of the actual system within the desired operating range because it incorporates the main features of the dynamics of the real plant. Of the controller performance, it can be observed that the desired response given by the reference model was tracked by the process response. The experimental tests corroborated the simulation results. The error signal was found to be bounded and small, and the control effort was also bounded, although the alleviation of chattering should be further studied. It is important to remark that the conventional PID with no robust tuning method is the scheme commonly used in these systems. The compared results also show that the adaptive controller is able to satisfactorily control the fluid level in the annular well, in spite of the presence of model uncertainties, unmodeled dynamics, parameter variations, and perturbations. Moreover, the results reveal that the control technique can improve production performance and reduce maintenance costs (for example, by avoiding fluid pound phenomenon).

Acknowledgements: The research was supported by the CTAI (facilities and infrastructure) at the Universidade Federal da Bahia.

References:

[1] W. L. Lake. *Petroleum Engineering Handbook*, volume 04. Society of Petroleum Engineers, Richardson, New York, USA, 2006.

[2] G. Takács. *Sucker-Rod Pumping Manual*. PennWell Books, Tulsa, USA, 2002.

[3] M. A. D. Bezerra, L. Schnitman, M. A. Barreto Filho, and J. A. M. Felippe de Souza. Pattern recognition for downhole dynamometer card in oil rod pump system using artificial neural networks. In *Proceedings of 11th International Conference on Enterprise Information Systems*, pages 351–355, Milan, Italy, May 2009. isbn: 978-989-8111-85-2.

[4] S. Petersen, P. Doyle, Carlsen, S., F. H. van der Linden, B. Myhre, M. Sansom, A. Skavhaug, E. Mikkelsen, and D Sjong. A survey of wireless technology for the oil and gas industry. *SPE Projects, Facilities and Construction*, 3(4):18, 2008. doi: 10.2118/112207-PA.

[5] B. Smith, M. Hall, A. Franklin, E. S. Johansen, nalmis, and H. Field-wide deployment of in-well optical flowmeters and pressure/temperature gauges at buzzard field. In *Proceedings of SPE Intelligent Energy Conference and Exhibition*, Amsterdam, The Netherlands, February 2008. Society of Petroleum Engineers. doi: 10.2118/112127-MS.

[6] E. van der Steen. Bsp: An evolution from smart wells to smart fields. In *Proceedings of Intelligent Energy Conference and Exhibition*, Amsterdam, The Netherlands, April 2006. Society of Petroleum Engineers. doi: 10.2118/100710-MS.

[7] I. H. Al-Arnaout, S. M. Al-Driweesh, and R. M. Al-Zarani. Wells to intelligent fields: Remotely operated smart well completions. In *Proceedings of Intelligent Energy Conference and Exhibition*, Amsterdam, The Netherlands, February 2008. Society of Petroleum Engineers. doi: 10.2118/112226-MS.

[8] H. Pinto, M. S. Silva, and G. Izetti. Integrated multizone low-cost intelligent completation. In *Proceedings of SPE Intelligent Energy Conference and Exhibition*, Amsterdam, The Netherlands, April 2006. Society of Petroleum Engineers. doi: 10.2118/99948-MS.

[9] F. Eldred, A. S. Cullick, S. Purwar, and S. Arcot. A small operator's implementation of a digital oil-field initiative. In *Proceedings of 2015 SPE Digital Energy Conference and Exhibition*, The Woodlands, USA, March 2015. Society of Petroleum Engineers. doi: 10.2118/173404-MS.

[10] L. A. Saputelli, C. Bravo, G. Moricca, R. Cramer, M. Nikolaou, C. Lopez, and S. Mochizuki. Best practices and lessons learned after 10 years of digital oilfield (dof) implementations. In *Proceedings of SPE Kuwait Oil and Gas Show and Conference*, Kuwait City, Kuwait, October 2013. Society of Petroleum Engineers. doi: 10.2118/167269-MS.

[11] G. V. Moisés, T. A. Rolim, and J. M. Formigli. Gedig: Petrobras corporate program for digital integrated field management. In *Proceedings of SPE Intelligent Energy Conference and Exhibition*, Amsterdam, The Netherlands, February 2008. Society of Petroleum Engineers. doi: 10.2118/112153-MS.

[12] M. Z. I. Ahmad, L. S. Colinus, M. S. Muzahidin, and M. K. Som. Samarang integrated operations (io) achieving well performance monitoring, surveillance and optimization through data and model driven workflows automation. In

Proceedings of 2015 SPE Digital Energy Conference and Exhibition, The Woodlands, USA, March 2015. Society of Petroleum Engineers. doi: 10.2118/173578-MS.

[13] L. A. Saputelli, M. Y. Khan, H. Chetri, R. Cramer, and S. Singh. Waterflood optimization and its impact using intelligent digital oil field (idof) smart workflow processes: A pilot study in sabriyah mauddud, north kuwait. In *Proceedings of 2014 International Petroleum Technology Conference*, Doha, Qatar, January 2014. Society of Petroleum Engineers. doi: 110.2523/17315-MS.

[14] K. Al-Yateem, M. Al-Amri, R. Ahyed, F. Aminzadeh, A. Althukair, and F. Al-Khelaiwi. Effective utilization of smart oil fields infrastructure towards optimal production and real time reservoir surveillance. In *Proceedings of 2014 International Petroleum Technology Conference*, Doha, Qatar, January 2014. Society of Petroleum Engineers. doi: 110.2523/17315-MS.

[15] E. Camponogara, A. Plucênio, A. F. Teixeira, and S. R. V. Campos. An automation system for gas-lifted oil wells: Model identification, control, and optimization. *Journal of Petroleum Science and Engineering*, 70:157167, 2010. doi:10.1016/j.petrol.2009.11.003.

[16] B. Ordoñez, A. Codas, and U. F. Moreno. Improving the operational conditions for the sucker-rod pumping system. In *Proceedings of IEEE International Conference on Control Applications*, pages 1259–1264, Saint Petersburg, Russia, July 2009. IEEE. doi: 10.1109/CCA.2009.5281122.

[17] B. Ordoñez, A. Codas, and U. F. Moreno. Sucker-rod pumping system: Simulator and dynamic level control using downhole pressure. In *Proceedings of 13th IEEE International Conference on Emerging Technologies and Factory Automation*, pages 282–289, Hamburg, Germany, September 2008. IEEE. doi: 10.1109/ETFA.2008.4638408.

[18] H. Zhou and D. Xu. Robust fault-tolerant tracking control scheme for nonlinear nonaffine-in-control systems against actuator faults. *WSEAS Transactions on Systems and Control*, 10(5):29–37, 2015. issn: 1991-8763 / e-issn: 2224-2856.

[19] T. Kim. Robust predictive control combined with an adaptive mechanism for constrained uncertain systems subject to disturbances. *WSEAS Transactions on Systems and Control*, 9(60):574–589, 2014. issn: 1991-8763 / e-issn: 2224-2856.

[20] L. H. S. Torres, L. Schnitman, and J. M. A. Felippe de Souza. Robust adaptive control of a sucker-rod pumping system of oil wells. In *Recent Advances in Circuits, Communications and Signal Processing: Proceedings of 12th WSEAS International Conference on Signal Processing, Robotics and Automation (ISPRA'13)*, pages 273–278, Cambridge, UK, February 2013. WSEAS. issn: 1790-5117 / isbn: 978-1-61804-164-7.

[21] R. Peterson, T. Smigura, C. Brunings, W. Quijada, and A. Gomez. A production increases at pdvsa using a improved srp control. In *Proceedings of SPE Annual Technical Conference and Exhibition*, San Antonio, USA, September 2006. Society of Petroleum Engineers. doi: /10.2118/103157-MS.

[22] M. de A. Barreto Filho. *Estimation of average reservoir pressure and completion skin factors of wells that produce using sucker rod pumping.* PhD thesis, The University of Texas at Austin, Austin, USA, 2001.

[23] J. E. Thomas, A. A. Triggia, C. A. Correia, C. V. Filho, J. A. D. Xavier, J. C. V. Machado, J. E. de S Filho, J. L. de Paula, N. C. M.de Rossi, N. E. S. Pitombo, P. C. V. de M. Gouvea, R. de S. Carvalho, and R. V. Barragan. *Fundamentos de Engenharia de Petrleo*. Ed. Intercilncia, Rio de Janeiro, Brasil, 2001.

[24] J. B. de Oliveira and A. D. Araújo. Indirect variable structure model reference adaptive control: Indirect vs-mrac. In *in Proceedings of XIV Brazilian Control Conference (CBA)*, pages 2557–2562, 2002. (in portuguese).

[25] L. Hsu and R. R. Costa. Variable structure model reference adaptive control using only input and output measurements part i. *International Journal of Control*, 49(2):349–416, 1989.

[26] J. B. de Oliveira and A. D. Araújo. Design and stability analysis of an indirect variable structure model reference adaptive control. *International Journal of Control*, 81(12):1870–1877, 2008. doi: 10.1080/00207170801918568.

[27] J. B. de Oliveira, A. D. Araújo, and S. M. Dias. Controlling the speed of a three-phase induction motor using a simplified indirect adaptive sliding mode scheme. *Control Engineering Practice*, 18(6):577–584, June 2010.

[28] K. Astrom and B. Wittenmark. *Adaptive Control*. Dover, New York, USA, 2008.

[29] P. A. Ioannou and J. Sun. *Robust Adaptive Control*. Prentice-Hall, New Jersey, USA, 1996.

[30] Y. Lim, R. Venugopal, and A. Galip Ulsoy. Auto-tuning and adaptive control of sheet metal forming. *Control Engineering Practice*, 20(2):156–164, 2012. doi: 10.1016/j.conengprac.2011.10.006.

[31] V. I. Utkin. *Sliding Modes and Their Application in Variable Structure Systems*. MIR, Moscow, Russia, 1978.